DELPHI Collaboration

DELPHI 2002-063 CONF 597
July 10, 2002

Search for a fourth generation b′-quark at LEP-II at $\sqrt{s} = 200 - 209$ GeV

Preliminary

S. Andringa[1], N. Castro[1], M. Espirito-Santo[1], P. Gonçalves[1], O. Oliveira[2], A. Onofre[1,3], M. Pimenta[1], B. Tomé[1] and F. Veloso[1]

[1]LIP-IST-FCUL, Av. Elias Garcia, 14, 1, P-1000 Lisboa, Portugal
[2]Dep. Física, Universidade de Coimbra, P-3004-516 Coimbra, Portugal
[3]UCP, R. Dr. Mendes Pinheiro, 24, P-3080 Figueira da Foz, Portugal

Abstract

A search for the double production of a fourth generation b'-quark was performed using data taken by the DELPHI detector at LEP-II. The analysed data were collected at centre-of-mass energies ranging from 200 to 209 GeV, with an integrated luminosity of about 344 pb^{-1}. No evidence for a signal was found. A preliminary upper limit on $\sigma_{e^+e^-\to b'b'} \times (BR_{b'\to bZ^0})^2$ of 0.2 pb was obtained at 95% confidence level for $m_{b'} = 100$ GeV.

Contributed Paper for ICHEP 2002 (Amsterdam)

1 Introduction

The number of light ($m < M_{Z^0}/2$) neutrino species, measured at LEP from the Z^0 decay widths [1], is :

$$N_\nu \;=\; 2.9841 \pm 0.0083\,. \tag{1}$$

However, the existence of additional generations of heavy leptons and quarks is not ruled out, either by the Standard Model (SM) or by experimental data. In some SM extensions, extra generations of fermions are predicted. A review of such models can be found in [2].

A fourth generation of fermions can be included in the SM by adding to the known fermionic spectrum another heavy family with the same quantum numbers. In the quark sector, an up quark, t', and a down quark, b', are included [3, 4]:

$$\begin{array}{c} Q = 2/3 \\ Q = -1/3 \end{array} \qquad \begin{pmatrix} u \\ d \end{pmatrix} \begin{pmatrix} c \\ s \end{pmatrix} \begin{pmatrix} t \\ b \end{pmatrix} \begin{pmatrix} \mathbf{t'} \\ \mathbf{b'} \end{pmatrix} \tag{2}$$

If kinematically allowed, the b'-quark may decay via charged currents (CC), $b' \to UW$, with $U = t', t, c, u$, or via flavour changing neutral currents (FCNC), $b' \to bX$, with $X = Z^0, \gamma, g$,H. In the SM, FCNC are absent at tree level, but can naturally appear at one-loop level, due to Cabbibo-Kobayashi-Maskawa (CKM) mixing. The smallness of the non-diagonal CKM matrix elements and the relative suppression of the loop contributions usually make FCNC cross-sections very small. However, if a fourth generation b'-quark exists and it is lighter than both the t' and the t, the leading CC decays $b' \to t'W$ and $b' \to tW$ are kinematically forbidden. It was pointed out by some authors [5, 6] that, due to double CKM suppression, the allowed CC would not be dominant. In this case, for high t' masses, the $b' \to bZ^0$ decay could be relevant [2, 6, 7, 8].

At LEP-I, all the experiments searched for the double production of b' [9, 10, 11, 12], giving a mass limit for the b'-quark close to half of the Z^0 mass. Searches for the double production of a b'-quark and subsequent FCNC decays in hadron colliders were performed by DØ [13] (for $m_{b'} < m_{Z^0} + m_b$) and CDF [14] (for $m_{b'} > 100$ GeV/c^2) at the TEVATRON. The most recent result comes from CDF, which gives an upper limit on $\sigma_{pp\to b'b'} \times (BR_{b'\to bZ^0})^2$ as function of the b' mass (for $100 < m_{b'} < 199$ GeV/c^2).

In this note the double production of b'-quarks with $m_{b'} = 100\,\mathrm{GeV}/c^2$, and subsequent FCNC decay, $b' \to bZ^0$, at LEP-II is considered. Different final state topologies are possible, corresponding to the different decay modes of the pair of Z^0 bosons. The channels in which one of the Z^0 bosons decays invisibly and the other decays into two quarks or two charged leptons were considered: $bZ^0bZ^0 \to b\nu\nu bll$ and $bZ^0bZ^0 \to b\nu\nu bjj$.

2 Data samples and event generators

The data were collected with the DELPHI detector [15] during the 1999 and 2000 LEP-II runs at $\sqrt{s} = 200-209$ GeV and correspond to a total integrated luminosity of 343.9 pb^{-1}. On September 1$^{\mathrm{st}}$ 2000, DELPHI suffered from a problem in a section of the Time Projection Chamber (TPC) — sector 6, which corresponded to 1/12 of the TPC acceptance. This required modifications of the pattern recognition and affected the quality of charged track reconstruction. Although the effect on the present analysis is small, these data

were analysed separately in order to control any systematic difference. The luminosity collected at each centre-of-mass energy is shown in table 1.

$\langle\sqrt{s}\rangle$ (GeV)	199.5	201.6	204.8	206.6	206.3 *
luminosity (pb^{-1})	82.7	40.2	80.0	81.9	59.2 *

Table 1: *Luminosity collected with the DELPHI detector at each centre-of-mass energy. The data collected during the year 2000 with the TPC fully operational were split into two energy bins, below and above* $\sqrt{s} = 206$ GeV, *with* $\langle\sqrt{s}\rangle = 204.8$ GeV *and* $\langle\sqrt{s}\rangle = 206.6$ GeV, *respectively.* (*) *The data collected with the sector 6 of the TPC turned off were analysed separately and have* $\langle\sqrt{s}\rangle = 206.3$ GeV.

SM background processes were generated at different centre-of-mass energies. All the four-fermion final states (both neutral and charged currents) were generated with WPHACT [16], while the $qq(\gamma)$ final state processes were generated with KK2F [17]. Processes giving mainly leptonic final states were also generated: Bhabha events with BHWIDE [18] and two-photon interactions with BDK (BDKRC) [19] for electron final states (other leptonic final states).

Signal samples were generated with PYTHIA 6.200 [20]. Although PYTHIA does not have FCNC decay channels for quarks, it is possible to activate them by modifying the decay products of an available channel. The resulting angular distributions for b' double production and decay were those predicted by the SM for any heavy down quark. An example of the angular distributions for b' (production) and b (decay) can be seen in figure 1. The generated events were separated in different samples, corresponding to different topologies and centre-of-mass energies. About one thousand events were generated for each centre-of-mass energy and topology: $b'b' \to b\nu\nu bjj$ and $b'b' \to b\nu\nu bll$, where l stands for any charged lepton.

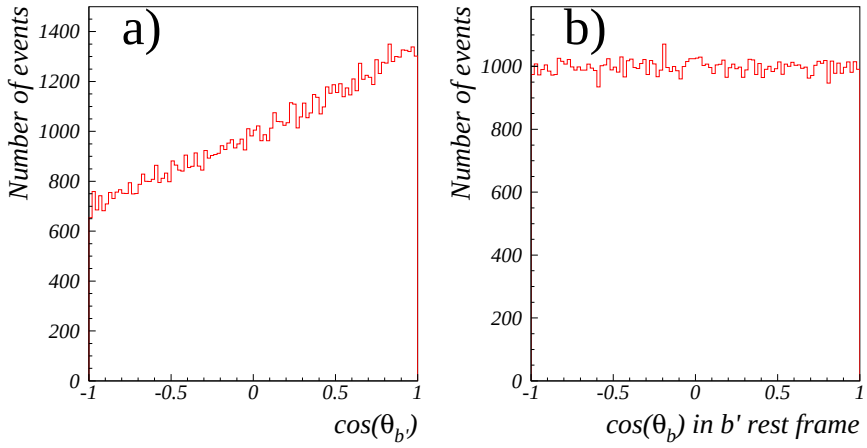

Figure 1: *Angular distributions (in* $\cos\theta$, *being* θ *the polar angle) of: a) the* b' *in the laboratory frame and b) the* b *(from* $b' \to bZ^0$*) in the* b' *rest frame. For these plots* 100 000 *events were generated with* $m_{b'} = 100$ *GeV and* $\sqrt{s} = 205$ *GeV.*

The generated signal and background events were passed through the detailed simulation of the DELPHI detector [15] and then processed with the same reconstruction and analysis programs as the real data. The number of simulated events of the different background processes were several times the number of the real data.

3 Analyses description

The b' pair production and FCNC decay through a Z^0 boson has been searched for in the $bb\nu\nu ll$ and $bb\nu\nu jj$ channels. These final states are characterized by the presence of a pair of low energy b jets, missing energy and a pair of energetic leptons or jets.

An initial event sample was obtained by requiring at least eight good charged tracks and a visible energy deposited above 20° in polar angle[1] greater than $0.2\sqrt{s}$. Isolated particles in the event were searched for by constructing double cones centered in the direction of charged tracks or neutral energy deposits. The energy inside an inner cone with half opening angle of 5° was required to be above 5 GeV, while the energy contained between the inner cone and the outer cone was required to be below 1 GeV, to ensure isolation. Both the opening angle of the outer cone and the total energy allowed between the two cones varied according to the topology of the event and to the energy and flavour identification of the reconstructed particle. For well identified photons or leptons, slightly looser criteria were used. The electron, photon and muon identification was based on the standard DELPHI algorithms [15, 22]. All the accepted events were forced into two or four jets (for $bbll\nu\nu$ and $bbjj\nu\nu$ topology, respectively) by the Durham jet algorithm [21].

3.1 $bbll\nu\nu$ topology search

The $bbll\nu\nu$ topology is characterized by the presence of two leptons and two low energy jets in the final state. Events with at least two isolated charged particles (according to the criteria described above) were selected.

Contamination from Bhabha events was reduced by requiring that at least one lepton[2] had $|\cos(\theta_{\rm lepton})| < 0.86$ and the energy of the second lepton had to be above 10 GeV, unless two well identified muons were found in the event. Only events with at least six good charged tracks with hits on the TPC were accepted.

The events were then separated in three groups, according to the lepton identification: events with two identified electrons (electron events), events with two identified muons (muon events) and events without two identified leptons of the same flavour (*no-id* events). In the *no-id* sample, only events with exactly two well isolated leptons and no isolated photons were kept.

Table 2 shows, at the end of the preselection, the number of data candidates, the expected number of SM background events and the signal efficiencies for the different centre-of-mass energies and leptonic flavours. The total signal efficiencies are between $(58 \pm 2)\%$ and $(62 \pm 2)\%$.

[1] In the standard DELPHI coordinate system, the z axis is along the electron direction and the polar angle is defined with respect to the z axis.

[2] Throughout this note the references to leptons are to be understood as references to the two most energetic isolated charged leptons. In addition, the leptons are assumed to be ranked by energy.

$\langle\sqrt{s}\rangle(GeV)$	e	μ	$(no\text{-}id)$
199.5	10 (6.4 ± 0.5) $\varepsilon = 21.2$	11 (10.0±0.5) $\varepsilon = 26.7$	50 (49.3±1.9) $\varepsilon = 11.3$
201.6	3 (3.1±0.2) $\varepsilon = 15.8$	2 (4.8±0.3) $\varepsilon = 28.4$	36 (23.5±0.9) $\varepsilon = 13.3$
204.8	8 (7.6 ± 0.6) $\varepsilon = 15.9$	9 (9.3±0.5) $\varepsilon = 27.9$	49 (46.8±1.7) $\varepsilon = 13.4$
206.6	6 (6.8±0.5) $\varepsilon = 18.0$	8 (10.0±0.6) $\varepsilon = 27.9$	50 (48.7±1.8) $\varepsilon = 11.5$
206.3	5 (5.1 ± 0.4) $\varepsilon = 16.6$	9 (6.6±0.4) $\varepsilon = 27.1$	37 (35.8±1.4) $\varepsilon = 10.7$

Table 2: *bbll$\nu\nu$ topology: number of selected events, expected background from SM processes (in brackets) and signal efficiency (%) for the different centre-of-mass energies and leptonic flavours after the preselection cuts. The signal efficiencies are not convoluted with* $BR_{Z^0Z^0\to ll\nu\nu}$.

Distributions of relevant variables are shown in figure 2 for data, SM background and signal, for all centre-of-mass energy bins. In figure 3 relevant distributions are shown separately for each leptonic sample.

After the preselection level, different cuts were applied to the electron, muon and *no-id* samples. In the electron sample, events were kept if the energy of the second electron was below 65 GeV, the angle between the two electrons was above 100° and the mass recoilling against the two jets was above 160 GeV/c^2. Events were kept in the muon sample if the angle between the two muons was above 125° and the missing energy was above 40 GeV. Finally, for the *no-id* sample, events were required to have:

- the energy of the second lepton below 50 GeV;
- the angle between the two leptons above 140°;
- the invariant mass of the two leptons above 10 GeV/c^2 and below 100 GeV/c^2;
- the momentum of the most energetic jet below 50 GeV/c and the momentum of the least energetic jet below 40 GeV/c;
- the recoil mass against the two jets above 140 GeV/c^2;
- the missing momentum below 70 GeV/c, the missing energy above 80 GeV and the polar angle of the missing momentum above 15° and below 165°;
- $-\log_{10}(y_{cut}(2 \to 1)) < 5$ and $-\log_{10}(y_{cut}(3 \to 2)) < 6$, where $y_{cut}(2 \to 1)$ and $y_{cut}(3 \to 2)$ are the Durham resolution variables in the transition from two to one jet, and from three to two jets, respectivelly.

Table 3 shows, after this selection, the number of data candidates, expected SM background and the signal efficiencies of the different centre-of-mass energies and leptonic flavours. The total signal efficiencies range from $(49 \pm 2)\%$ to $(53 \pm 2)\%$. The branching ratio for $Z^0Z^0 \to ll\nu\nu$ is about 4%.

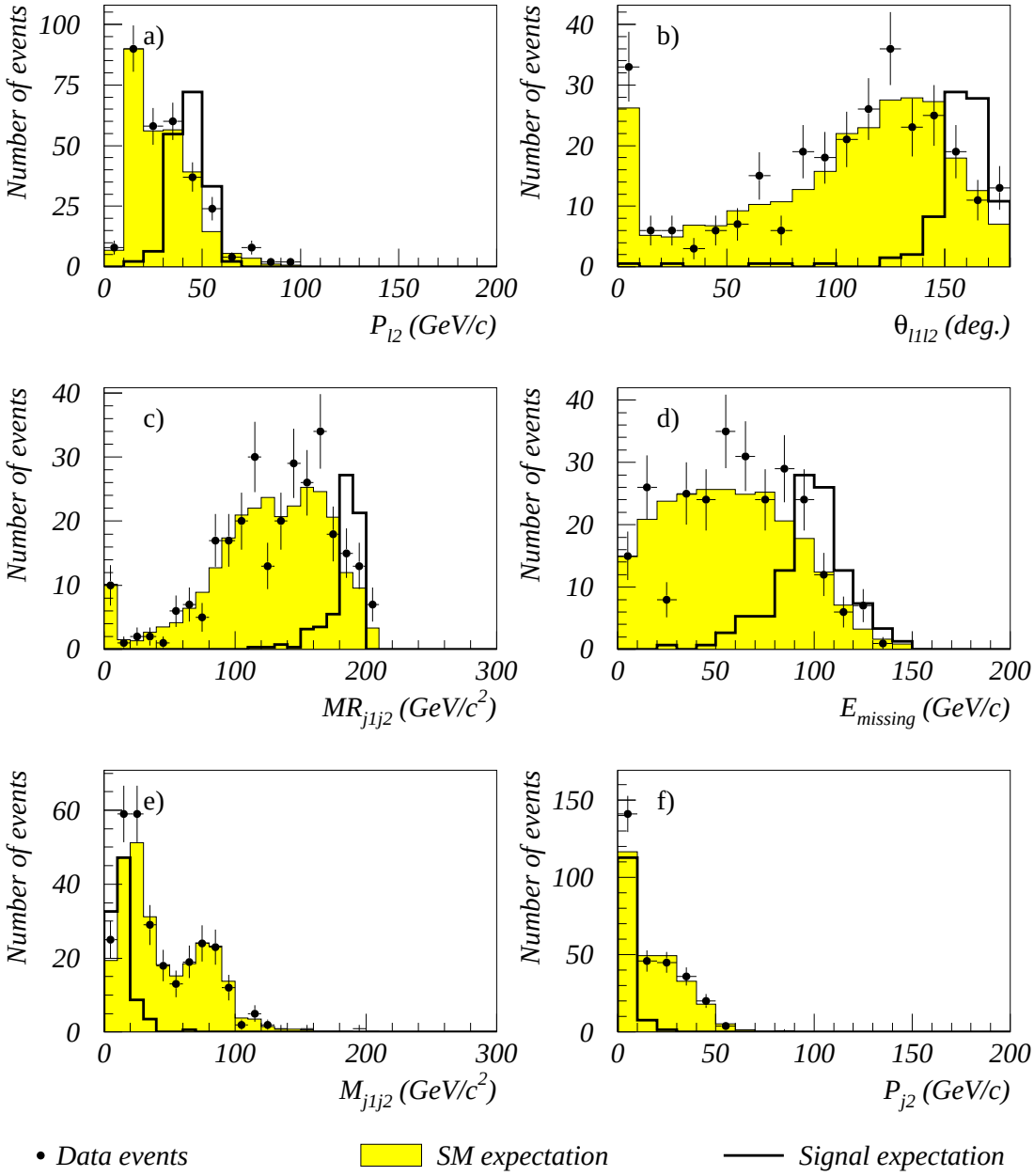

Figure 2: *bbllνν topology: comparison of data and simulation, at the preselection level and for all centre-of-mass energies ($\sqrt{s} = 200 - 209$ GeV), for a) the momentum of the second lepton; b) the angle between the two leptons; c) the recoil mass against the two jets system; d) the missing energy; e) the two jet invariant mass and f) the momentum of the least energetic jet. Signal ($m_{b'} = 100$ GeV/c^2) is also shown with arbitrary normalization.*

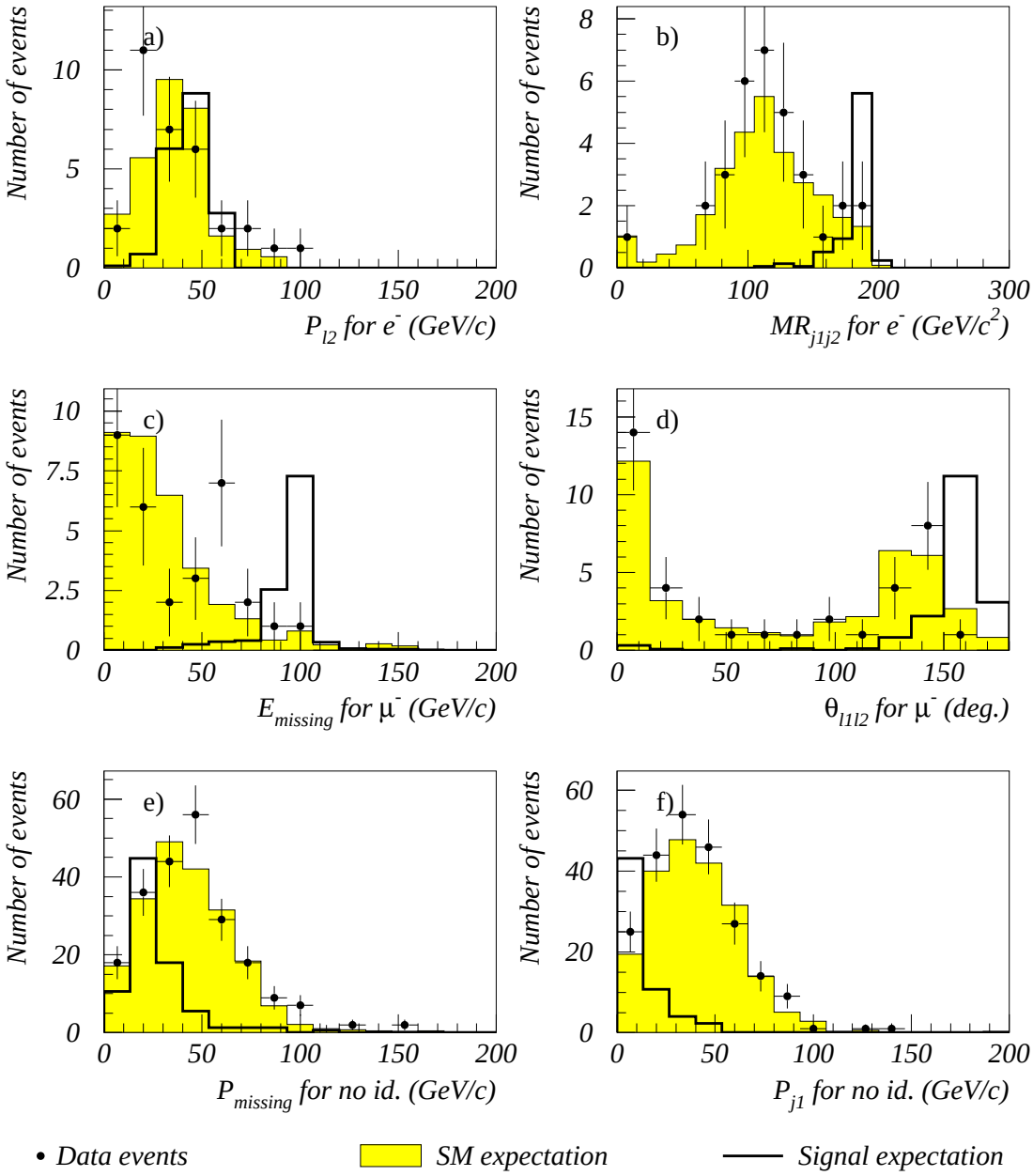

Figure 3: *bbllνν topology: comparison of data and simulation, at the preselection level and for all centre-of-mass energies ($\sqrt{s} = 200 - 209$ GeV), for the electron sample of a) the momentum of the second lepton and b) the recoil mass against the two jets system. For the muon sample: c) the missing energy and d) the angle between the two leptons. For the* no-id *sample: e) the missing momentum and f) the momentum of the most energetic jet. Signal ($m_{b'} = 100$ GeV/c^2) is also shown with arbitrary normalization.*

$\langle\sqrt{s}\rangle$ (GeV)	e	μ	(no-id)
199.5	0 (0.5±0.2) $\varepsilon = 19.9$	1 (0.3±0.1) $\varepsilon = 24.9$	2 (1.0±0.2) $\varepsilon = 5.9$
201.6	0 (0.2±0.1) $\varepsilon = 14.8$	0 (0.2±0.1) $\varepsilon = 27.6$	2 (0.5±0.2) $\varepsilon = 8.6$
204.8	0 (0.6±0.1) $\varepsilon = 14.4$	0 (0.4±0.1) $\varepsilon = 26.3$	0 (1.1±0.3) $\varepsilon = 7.9$
206.6	0 (0.4±0.1) $\varepsilon = 16.9$	0 (0.5±0.2) $\varepsilon = 26.2$	3 (1.4±0.4) $\varepsilon = 7.6$
206.3	0 (0.2±0.1) $\varepsilon = 15.2$	0 (0.2±0.1) $\varepsilon = 25.8$	0 (1.4±0.2) $\varepsilon = 6.6$

Table 3: *$bbll\nu\nu$ topology: number of selected events, expected background from SM processes (in brackets) and signal efficiency (%) for the different centre-of-mass energies and leptonic flavours at the final selection level. The signal efficiencies are not convoluted with* $BR_{Z^0Z^0\to ll\nu\nu}$.

3.2 $bbjj\nu\nu$ topology search

The $e^+e^- \to b'b' \to bjjb\nu\nu$ topology is characterized by the presence of four jets in the final state and about 90 GeV of missing energy. In order to select this topology a discriminant analysis was used. In the preselection level events were required to have:

- at least 20 good tracks;
- a visible momentum above 20° in polar angle greater than $0.2\,\sqrt{s}/c$;
- no isolated photons or leptons;
- a transverse visible energy above $0.15\,\sqrt{s}$;
- the leading (i.e. most energetic) particle of the most energetic jet with an energy below $0.1\,\sqrt{s}$ and a tranverse momentum per track below $0.1\sqrt{s}/c$;
- a momentum associated to rejected tracks[3] below $0.2\,E_{vis}/c$, where E_{vis} is the visible energy above 20° in polar angle.

Figure 4 shows, at this level and for the 206.6 GeV centre-of-mass energy bin, some relevant distributions for data, expected SM background and signal.

In a second stage of selection, $q\bar{q}$ background was reduced by requiring:

- the polar angle of the direction of the missing momentum above 30° and below 150°;
- $(h_1{+}h_3)$ below 0.5 and $(h_2{+}h_4)$ below 1.2, where $h_{i=1,4}$ are the first four Fox-Wolfram normalized momenta [23];
- the Durham resolution variable in the transition from four to three jets, $y_{cut}(4 \to 3)$, above 0.001;
- the Narrow Jet Broadening [24] above 0.08;
- the acollinearity[4] below 50°.

[3]Rejected tracks are charged tracks not passing the track selection, which basically requires a momentum above 0.1 GeV/c with a relative error below 1, and impact parameters along the beam direction and in the transverse plane below 4 cm and below 4 cm/$\sin\theta$ respectively (θ is the polar angle).

[4]The acollinearity is defined as $180 - \theta_{j1\,j2}$, where $\theta_{j1\,j2}$ is the angle between the two most energetic jets (in degrees).

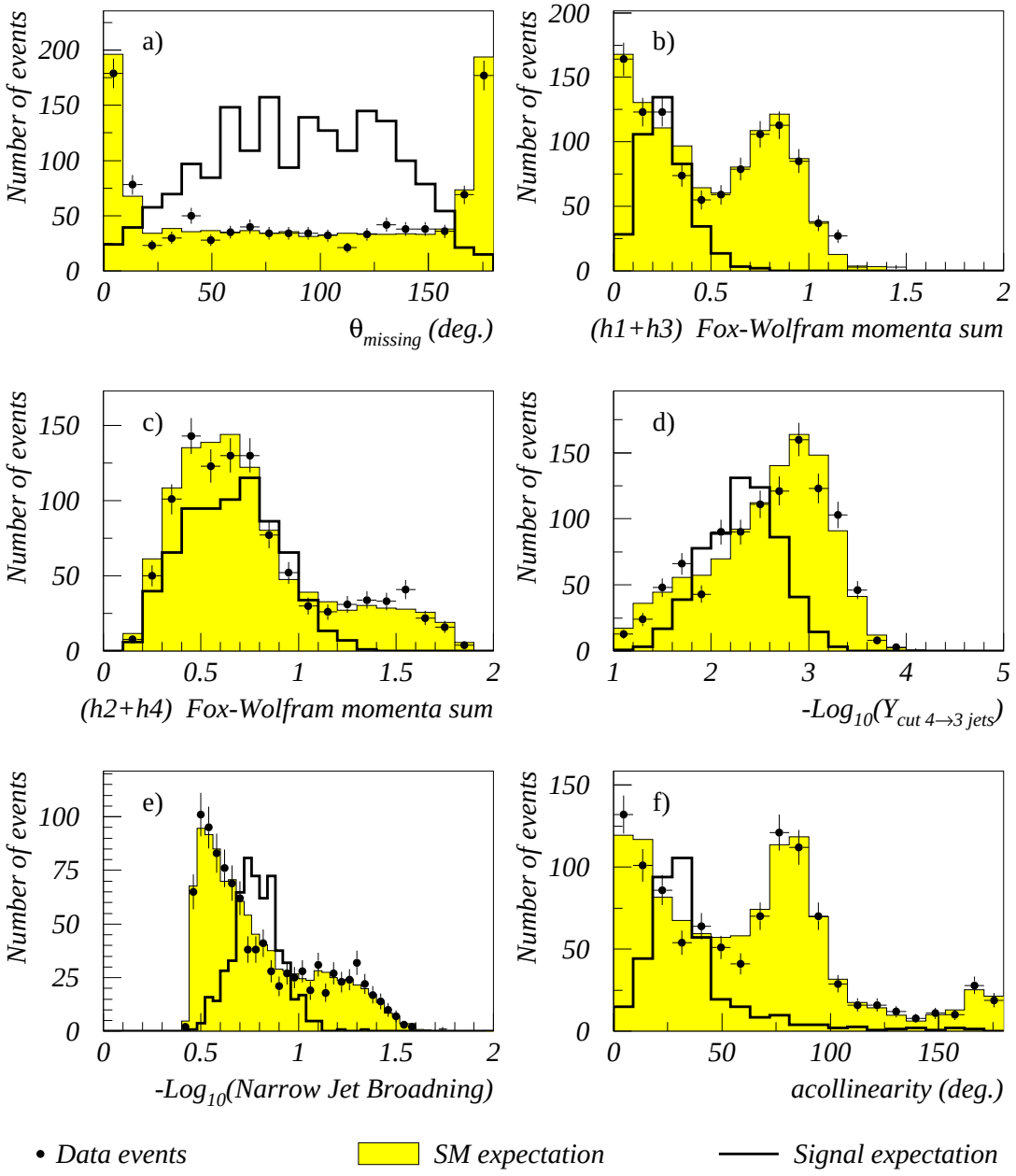

Figure 4: *bbjjνν topology: comparison of data and simulation, at preselection level and for the* $\sqrt{s} = 206.6$ GeV *bin, of a) the polar angle of the missing momentum; b) the* $(h1+h3)$ *Fox-Wolfram momenta sum; c) the* $(h2+h4)$ *the Fox-Wolfram momenta sum; the d)* $-\log_{10}[y_{cut}(4 \to 3)]$*; e) the* $-\log_{10}$ *(Narrow Jet Broadening) and f) the acollinearity. Signal* ($m_{b'} = 100$ *GeV*$/c^2$) *is also shown with arbitrary normalization.*

$\langle\sqrt{s}\rangle$ (GeV)	DATA (SM EXPECTATION)		signal efficiency (%)	
	preselection	$q\bar{q}$ reduction cuts	preselection	$q\bar{q}$ reduction cuts
199.5	1215 (1172.2±13.2)	153 (161.3±4.0)	63.6	42.0
201.6	552 (557.8±6.3)	63 (76.7±1.9)	61.8	41.3
204.8	999 (1088.6±12.2)	139 (157.1±3.8)	62.0	42.3
206.6	1051 (1086.4±12.1)	151 (156.1±3.8)	59.8	40.0
206.3	698 (776.6±8.9)	93 (114.8±2.8)	59.0	38.9

Table 4: *$bbjj\nu\nu$ topology: number of selected events and expected background from SM processes for different centre-of-mass energies at each selection level. The corresponding signal efficiencies (%) are also shown. These efficiencies are not convoluted with $BR_{Z^0Z^0\to jj\nu\nu}$.*

Table 4 shows, for each of the selection levels and the different centre-of-mass energies, the number of data candidates, expected SM background events and the signal efficiencies. The uncertainties in the efficiency are about 2%. The branching ratio $BR_{Z^0Z^0\to jj\nu\nu}$ is about 28%.

For the selected events, a signal likelihood ($\mathcal{L}_S$) and a background likelihood ($\mathcal{L}_B$) were constructed using probability density functions based on the following variables:

- $A^{jj}_{cop} \times \min(\sin\theta_1, \sin\theta_2)$, where A^{jj}_{cop} is the acoplanarity (defined in the plane transverse to the beam) and $\theta_{1,2}$ are the polar angles of the first and second jets (with the events forced into two jets[5]);
- sphericity of the event;
- χ^2 of the kinematic fit imposing energy-momentum conservation to the 4-jets system;
- angle between the two jets that best reconstruct the W mass (for WW background rejection).

These variables are shown in figure 5 for data, expected background and signal at $\sqrt{s} = 206.6$ GeV bin. The discriminant variable was defined as the $\log_{10}(\mathcal{L}_S/\mathcal{L}_B)$. As an example, $\log_{10}(\mathcal{L}_S/\mathcal{L}_B)$ for data, SM expectation and signal for the $\sqrt{s} = 206.6$ GeV bin are shown in figure 6-a. In figure 6-b the number of data candidates, SM expectation and the signal efficiency (convoluted with the branching ratio $BR_{Z^0Z^0\to jj\nu\nu} \sim 28\%$) are plotted as function of the cut in the discriminant variable. The full distribution of the discriminant variable was used in the evaluation of the results of this note. At this level some deficit in data with respect to the SM expectation is observed. This effect is concentrated at low values of the χ^2 distribution. No significant deficit is observed at high values of this variable, which dominate the signal-like region of the likelihood ratio.

[5]While the four jets topology characterizes the signal, the two jets configuration is used in the background rejection.

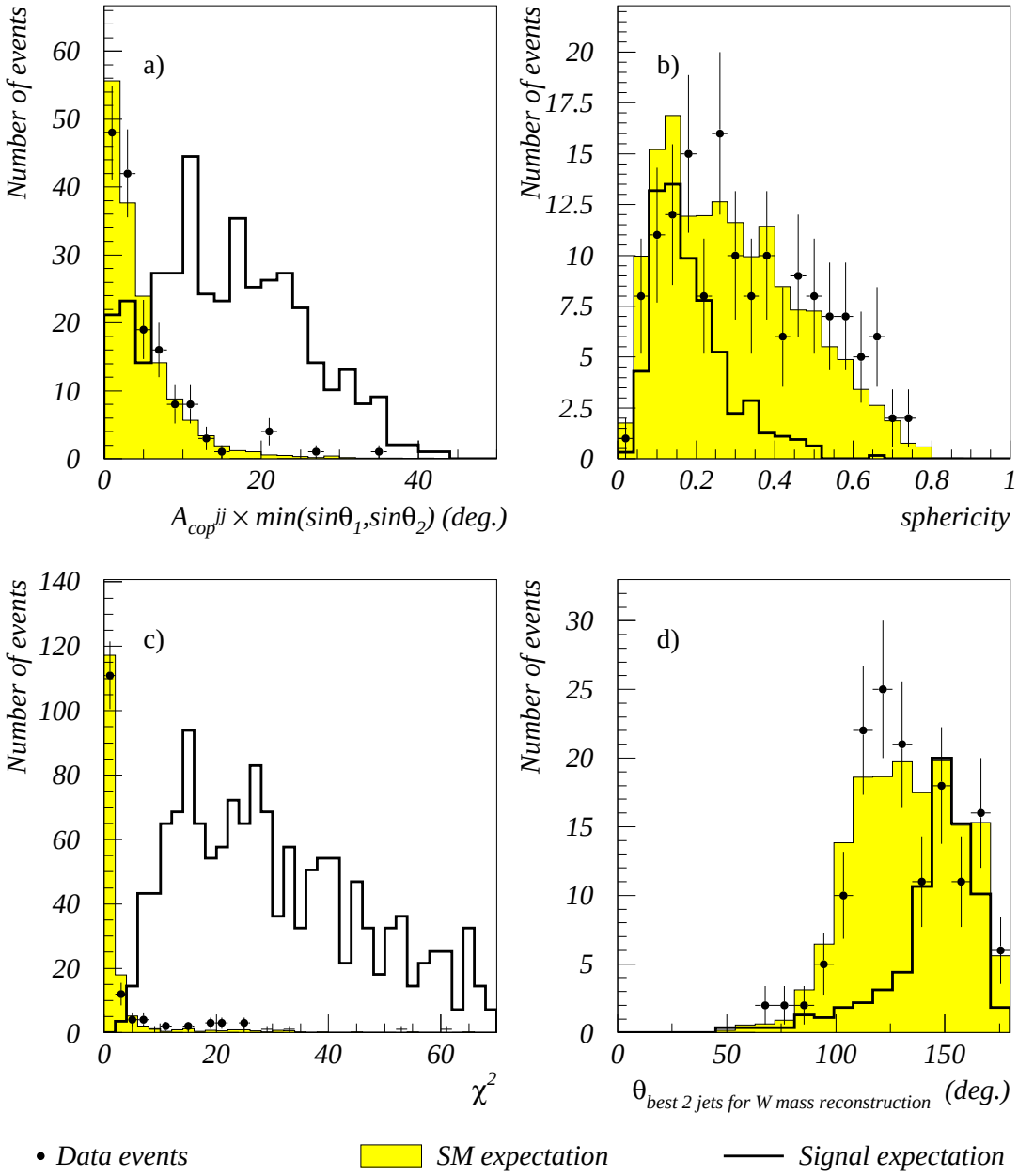

Figure 5: *bbjjνν topology: comparison of data and simulation, after the $q\bar{q}$ reduction cuts, at $\sqrt{s} = 206.6$ GeV bin, of a) the $A_{cop}^{jj} \times \min(\sin\theta_1, \sin\theta_2)$, where A_{cop}^{jj} is the acoplanarity and $\theta_{1,2}$ are the polar angles of the first and second jets; b) the sphericity; c) the χ^2 of the kinematic fit imposing energy momentum conservation to the 4-jets system d) the angle between the two jets that best reconstruct the W mass. Signal ($m_{b'} = 100\ GeV/c^2$) is also shown with arbitrary normalization.*

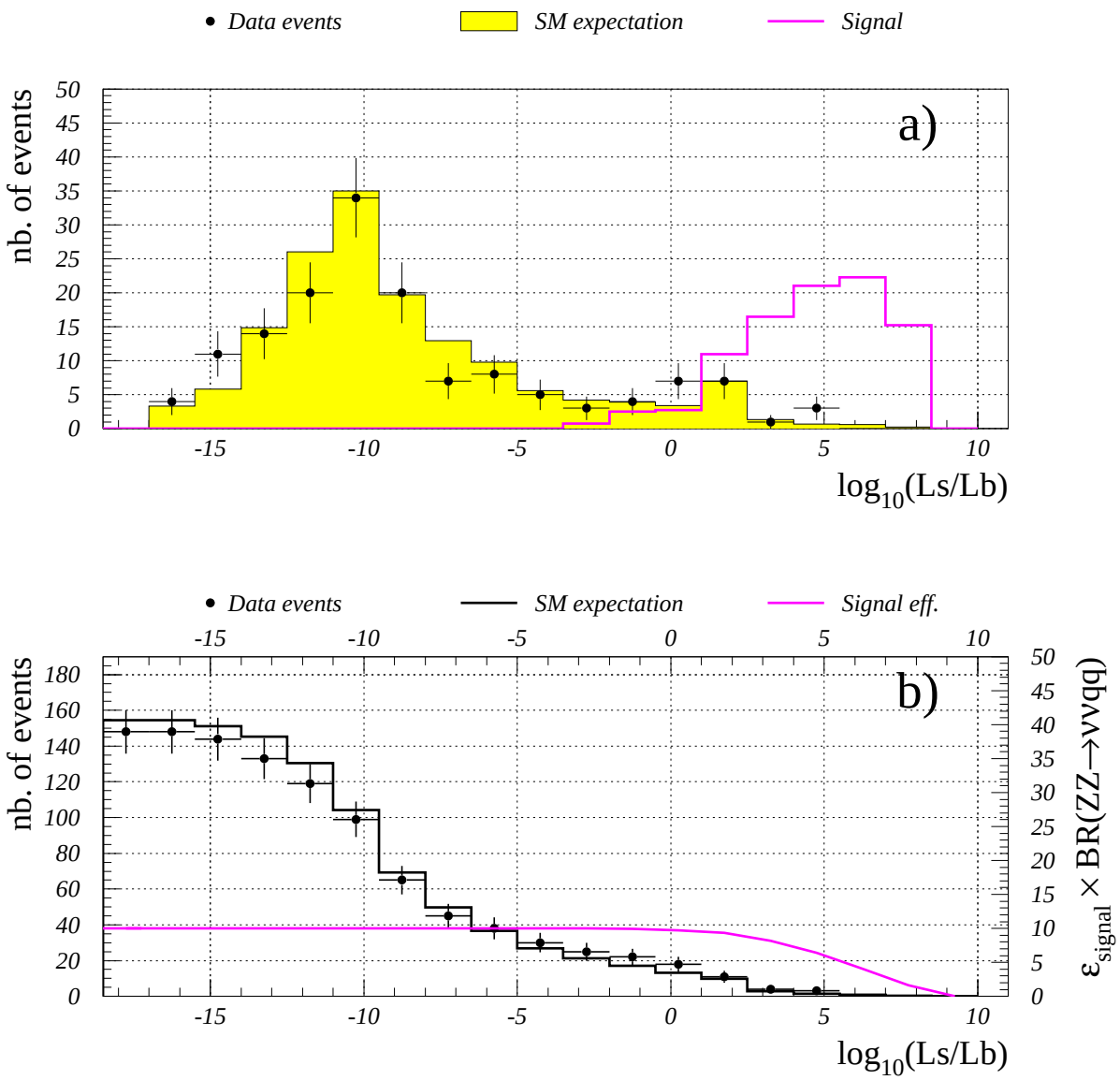

Figure 6: *topology bbjjνν:* a) *the discriminant variable,* $\log_{10}(\mathcal{L}_S/\mathcal{L}_B)$*, for selected events, expected SM background and signal* ($m_{b'} = 100$ *GeV) for* $\sqrt{s} = 206.6$ GeV *bin. The signal normalization is arbitrary;* b) *the number of selected events, expected background from SM processes and signal efficiency convoluted with the* $BR_{Z^0Z^0\to jj\nu\nu}$*, as function of the cut on the discriminant variable,* $\log_{10}(\mathcal{L}_S/\mathcal{L}_B)$*, for* $\sqrt{s} = 206.6$ *GeV bin. The* $BR_{Z^0Z^0\to jj\nu\nu}$ *is about 28%.*

4 Results and conclusion

The data collected with the DELPHI detector at centre-of-mass energies ranging from 200 GeV to 209 GeV show no evidence for the double production of a fourth generation b'-quark with $m_{b'} = 100$ GeV. Preliminary limits on $\sigma_{e^+e^-\to b'b'} \times (BR_{b'\to bZ^0})^2$ were obtained (at 95% confidence level) using the method described in [25]. The observed and expected limits for each of the considered channels, and the combined limits are shown in table 5. The combined result gives an upper limit on $\sigma_{e^+e^-\to b'b'} \times (BR_{b'\to bZ^0})^2$ of 0.19 pb. Conservatively, a systematic error of 15% was attributed to the background when deriving the limits. No directly comparable (i.e. from leptonic colliders) limits on $\sigma_{e^+e^-\to b'b'} \times (BR_{b'\to bZ^0})^2$ were found in the literature.

upper limits on $\sigma_{e^+e^-\to b'b'} \times (BR_{b'\to bZ^0})^2$ (pb) for $m_{b'} = 100$ GeV		
$bbll\nu\nu$ topology	$bbjj\nu\nu$ topology	combined result
0.65 (0.80)	0.26 (0.29)	0.21 (0.26)

Table 5: *Observed and expected (in brackets) limits on* $\sigma_{e^+e^-\to b'b'} \times (BR_{b'\to bZ^0})^2$ *at 95% confidence level.*

References

[1] ALEPH, DELPHI, L3 and OPAL coll., Abbaneo D et al., CERN-EP-2001-098 (2001).

[2] Frampton P. H., Hung P.Q. and Sher M., *Phys. Rep.* **330** (2000) 263.

[3] Djouadi A., Ng. J. and Rizzo T. in *Electroweak symmetry breaking and new physics at the TeV scale*, ed. Barklow, Timothy - World Scientific, Singapore (1997).

[4] Novikov V.A. and Okun L.B., *Extra generations and discrepancies of electroweak precision data*, hep-ph/0111028 (2002).

[5] Hou W.S. and Stuart R.G., *Phys. Rev. Lett.* **89** (1989) 617.

[6] Hou W.S. and Stuart R.G., *Nucl. Phys.* **B349** (1991) 91.

[7] Sher M., *Phys Rev.* **D61** (2000) 057303.

[8] Arhrib A. and Hou W.S., *Phys Rev.* **D64** (2001) 073016.

[9] ALEPH Coll., Decamp D. et al., *Phys. Lett.* **B236** (1990) 511.

[10] OPAL Coll., Akrawy M.Z. et al., *Phys. Lett.* **B246** (1990) 285.

[11] DELPHI Coll., Abreu P. et al., *Nucl. Phys.* **B367** (1991) 511.

[12] L3 Coll., Adriani et al., *Phys. Rep.* **236** (1993) 1.

[13] DØ Coll., Abachi S. et al., *Phys. Rev. Lett.* **78** (1997) 3818.

[14] CDF Coll., Affolder T. et al., *Phys. Rev. Lett.* **84** (2000) 835.

[15] DELPHI coll., Aarnio P. et al., *Nucl. Instr. Meth.* **A303** (1991) 233;
DELPHI coll., Abreu P. et al., *Nucl. Instr. Meth.* **A378** (1996) 57.

[16] Accomando E. and Ballestero, *Comp. Phys. Comm.* **99** (1997) 270.

[17] Jadach S., Ward B.F.L. and Was Z., *Comp. Phys. Comm.* **130** (2000) 260.

[18] Jadach S., Płaczek W. and Ward B.F.L., *Phys. Lett.* **B390** (1997) 298.

[19] Berends F. A. et al., *Comp. Phys. Comm.* **40** (1986) 271, 285 and 309.

[20] Sjöstrand T. et al., *Comp. Phys. Comm.* **135** (2001) 238.

[21] Catani S. et al., *Phys. Lett.* **B269** (1991) 432.

[22] Cossutti et al., "REMCLU: a package for the Reconstruction of Electromagnetic CLUsters at LEP200", DELPHI Note 2000-164 PROG 242.

[23] Fox G. and Wolfram S., *Phys. Lett.* **B82** (1979) 134.

[24] Nason P. et al., in *Physics at LEP2 — Vol. 1*, ed. Altarelli G, Sjöstrand T. and Zwirner F. - CERN report 96-01 (1996) 249.

[25] DELPHI coll., Read A.L., DELPHI 97-158 PHYS 737 (1997);
Read A.L., CERN report 2000-005 (2000) 81.